Current Trends in Biotechnology and Pharmacy
Vol. 17(4) 1496-1505,October 2023, ISSN 0973-8916 (Print), 2230-7303 (Online)
DOI: 10.5530/ctbp.2023.4.83

In silico Molecular Docking and Scrutinizing Druglike Properties of Selected Phytoconstituents Against TAK1, Xanthin Oxidase, and IL-1 β Targets in Gouty Arthritis

Yasir K Mahdi*[1], Mogana R*[1] , Dharmendra Kumar*[2] , Arijit Nandi[3], Anwesha Das[4], Yasir A Atia[5], Rajeev Ranjan[2], YaduNandan Dey[3]

[1]Faculty of Pharmaceutical Sciences, UCSI University, Kuala Lumpur, Malaysia 56000.
[2]Narayan Institute of Pharmacy, Gopal Narayan Singh University, Jamuhar, Sasaram, Rohtas, Bihar,821305
[3]Dr B. C Roy College of Pharmacy and Allied Health Sciences, Durgapur-713206, West Bengal.
[4]Department of Medicinal Chemistry, NIPER, Ahmedabad, Gujarat, 382355
[5]Department of Biochemistry, Al Kindy College of Medicine, Baghdad University, Iraq.
*Corresponding author: yasirkmahdi@gmail.com

Abstract

Common manifestation of gout is deposition of monosodium urate crystals in joints followed by cytokinine-induced inflammatory responses. Xanthin Oxidase (PDB ID: 3NVY) and proinflammatory cytokinines, eg., TAK1 (PDB ID: 7NTH) and IL-1 β (PDB ID: 5R8Q) are vastly accountable for the severity of the disease. Inhibition of these targets with phytoconstituents would be preferable option in the treatment of gout patients. In the present study, *in silico* molecular docking analysis of Orientin, Vitexin, Apigenin, and Harman were performed using Glide XP, Schrodinger 2017_2, with above drug targets to investigate docking score, binding free energies and druggability. The results revealed a docking score and binding energy in the range of -11.862 kcal/mol to -3.130 kcal/mol and -53.282 kcal/mol to -32.346 kcal/mol respectively. Except Harman all the compounds have considerable docking score and binding energies, which typically indicate that they have the optimum interaction with the binding sites. ADME/T analysis performed using QikProp program of Schrödinger 2017-2 and the SwissADME online server indicated that the Vitexin and Apigenin have the physiochemical properties to be developed as drugs. These studies can be used to develop alternate therapeutic options for the treatment of gout.

Keywords: Gout, Molecular docking, TAK1, Xanthin oxidase, IL-1 β, Phytoconstituents

Introduction

Arthritis caused by gout is a major disability of joints in the elderly population and accounts for millions of outpatient visits in the clinics (1). This painful condition occurs due to the inflammatory reaction, when monosodium urate crystallizes within the joints (2). Although the exact etiology of the disease is not known, the association between crystal deposition and inflammation of the joints have been well documented in the past (3, 4). Molecular pathophysiology of the gout reveals the involvement of variety of molecules, including cell surface receptors, signalling proteins and/or transcription factors in the cascade of cytokinine-induced inflammation and tissue injury (5, 6). The role of Xanthin Oxidase inhibitors in the management of gout associated with hyperuricemia is established clinically, since half a century ago. These attenuate the catalysis by Xanthin oxidase to produce uric acid and reactive oxygen species (7). Recently few novel drug targets for the treatment of gouty arthritis have been iden-

tified, which upon pharmacological inhibition ameliorate the symptoms. Of these, the prominent signalling factors are transforming growth factor β activated kinase-1 (TAK1) and interleukin-1 beta (IL-1 β). TAK1 is activated midway in the signal transduction pathways in response to various inflammatory cytokines. Owing to its position in the signalling cascade i.e., upstream to mitogen-activated protein kinases and the IkB kinase complex, TAK1 may be considered as attractive drug target (8-12). In gout at the site of crystal deposition, release and activation of proinflammatory cytokines like IL-1 β triggers cardinal inflammatory response with vasodilatation and rapid recruitment of neutrophils, predisposing acute inflammatory response (13). Sustained IL1β secretion can result in the production of matrix degrading enzymes that break down cartilage and bone, thereby augmenting the symptoms (14).

Manipulating these drug targets with chemical drug can be effective, but may be expensive, develop resistance and led to many side effects. Hence, identification of phytoconstituents with TAK1, Xanthin Oxidase, and IL-1 β inhibitory potential can be an important breakthrough in the treatment of gouty arthritis. Here, we report the first *In silico* study to find the binding potential and druglike properties of four selected phytoconstituents (eg. Orientin, Vitexin, Apigenin, and Harman). The results from this study can be a foundation for developing new alternative therapy for gouty arthritis.

Material and Methods

In silico studies

Molecular docking

The crystal structure of TAK1 (PDB ID: 7NTH) (15), Interleukin-1 beta (PDB ID: 5R8Q) (16), and Bovine Xanthine Oxidase (PDB ID: 3NVY) (17), were extracted from the RCSB Protein Data Bank (PDB). All the crystallized protein structures were then prepared using the Protein Preparation Wizard module in Schrodinger 2017_2 (18) to remove all the water molecules (in case of co-crystallized ligand bound protein i.e. 7NTH, 5R8Q, and 3NVY water molecules remained only beyond 5 Å from the ligand molecule), missing side chains, missing loops, and hydrogen atoms were added, protonation states and partial charges were assigned using the OPLS3 force field. After that, all the protein structures were restrained-minimized until the root-mean-square deviation (RMSD) of the non-H atoms converged to 0.3 Å. The structures of the of Orientin, Vitexin, Apigenin, and Harman were retrieved from the PubChem database, and prepared using the LigPrep module of Schrodinger 2017-2 suite to generate tautomers, the chiralites were retained and the ionization state at pH 7.0±2.0 was determined using Epik (19). Using the prepared and minimized receptor structures, the receptor grids were generated either around the co-crystallized-ligand site of the crystal structure. Then, the Orientin, Vitexin, Apigenin, and Harman were docked with the proteins using the Glide XP protocol (20).

Molecular dynamics

The docked complexes of the protein-ligand were simulated in the Desmond module of Schrodinger software. An orthorhombic box was built using a system builder panel. Simple point charge model was used as a water model for the simulation of the docked ligand-protein complex. The constant-temperature, constant-pressure ensemble (NPT) was used for the MD Simulation at a temperature of 310 K and an atmospheric pressure of 1.013 bar for 50 ns. The output of the molecular dynamics studies was studied in detail using the Simulation Interactions Diagram Report of the Desmond software (21, 22).

In silico physico-chemical and ADME/T studies

Qikprop module of Schrödinger suite 2017-2 (QikProp, 2017_2) and SwissADME were used to determine the physico-chemical and ADME/T properties of the best two molecules which helps to determine the physico-chemical significant descriptors and phar-

macokinetically important properties of the molecules. For the fast assessment of the physico-chemical and ADME/T properties of the Orientin, Vitexin, Apigenin, and Harman it was discussed in the results section.

Results and Discussion

Molecular docking analysis

Molecular docking studies of Orientin, Vitexin, Apigenin, and Harman were performed using Glide XP, Schrodinger 2017_2 and the energy minimized structures of the ligands were docked into the crystal structure of TAK1 (PDB ID: 7NTH, resolution of 1.97 Å), Interleukin-1 beta (PDB ID: 5R8Q, resolution of 1.23 Å), and Bovine Xanthine Oxidase (PDB ID: 3NVY, resolution of 2.00 Å) with validated grid parameters. The Glide XP docking scores and the amino acid residues responsible for the interactions were listed in Table 1 respectively. Based on the docking scores, the compounds' 3D and 2D interaction diagrams were analysed for the proposed activity. The molecular mechanics-generalized Born surface area (MMGBSA) method was used to calculate the binding free energy.

The four phytoconstituents shows considerable docking score and binding free energy against the PDB ID: 7NTH were found to be Orientin (-11.862 kcal/mol, -46.669 kcal/mol), Vitexin (-11.844 kcal/mol, -53.282 kcal/mol), Apigenin (-9.277 kcal/mol, -49.012 kcal/mol), and Harman (-5.587 kcal/mol, -38.578 kcal/mol). Except Harman, all the compounds had the docking score of above -8.000 kcal/mol, which typically indicate that they have the optimum interaction with the binding site. Val 42, Arg 44, and Ala 107 were the amino acids responsible for the H-bond formation. Val 42, Ala 46, Ala 61, Val 90. Met 104, Tyr 106, Ala 107, Pro 160, Leu 163, Cys 17 were the most common amino acids which are accountable for the hydrophobic interactions. Ser 111 was responsible for the polar interaction with the two best docking score containing Orientin and Vitexin. Harman is able to form a Pi-pi stacking interaction with the Tyr 106 as shown in Figure1.

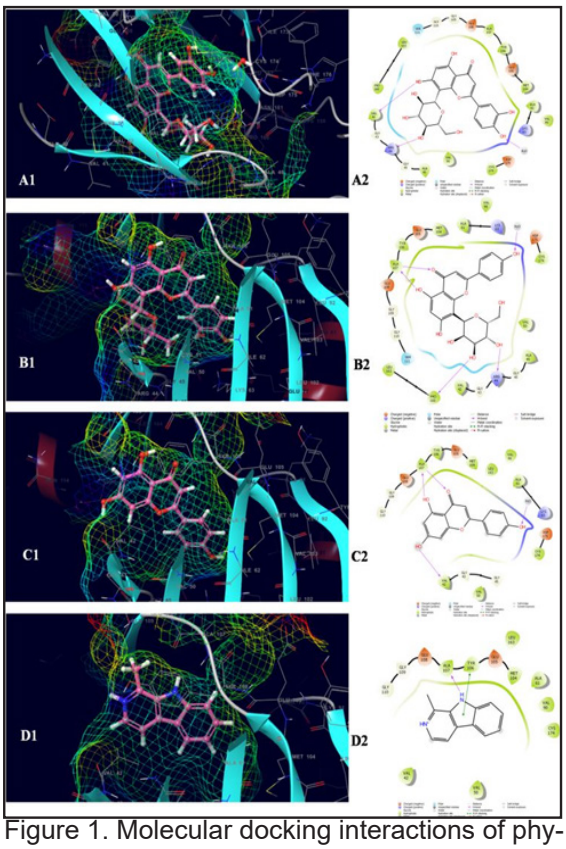

Figure 1. Molecular docking interactions of phytoconstituents in the binding pocket of PDB ID: 7NTH. (3D and 2D representation of Orientin (A1, A2), Vitexin (B1, B2), Apigenin (C1, C2), and Harman (D1, D2) in the binding pocket of (PDB ID: 7NTH))

The four phytoconstituents shows considerable docking score and binding free energy against the PDB ID: 5R8Q were found to be Orientin (-7.078 kcal/mol, 44.091 kcal/mol), Vitexin (-7.029 kcal/mol, -44.036 kcal/mol), Apigenin (-5.293kcal/mol, -39.896 kcal/mol) and Harman (-3.130 kcal/mol, -32.346 kcal/mol). The most common H-bond forming amino acids were Tyr 24 and Glu 25 while Pro 23, Tyr 24, Leu 26, Leu 80, Leu 82, Val 132, and Phe 133 were the most common amino acids accountable for the hydrophobic interactions. Ser 21, Thr 79, and Gln 81 were found to be responsible for the polar interactions (Figure 2).

Current Trends in Biotechnology and Pharmacy
Vol. 17(4) 1496-1505,October 2023, ISSN 0973-8916 (Print), 2230-7303 (Online)
DOI: 10.5530/ctbp.2023.4.83

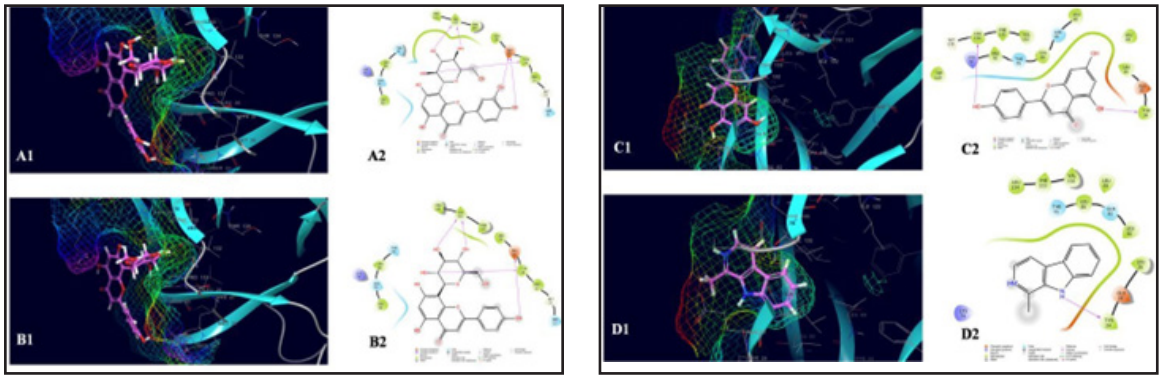

Figure 2. Molecular docking interactions of phytoconstituents in the binding pocket of PDB ID: 5R8Q. (3D and 2D representation of Orientin (A1, A2), Vitexin (B1, B2), Apigenin (C1, C2), and Harman (D1, D2) in the binding pocket of (PDB ID: 5R8Q))

Table 1. Molecular docking results of the compounds based on their docking scores and interactions

PDB ID	Compound Name	Glide score (Kcal/mol)	MM-GBSA dG Bind (Kcal/mol)	H-bond forming residues	Hydrophobic interaction forming residues	Polar interaction forming residues
7NTH	Orientin	-11.862	-46.669	Val 42, Arg 44	Val 42, Ala 46, Ala 61, Val 90. Met 104, Tyr 106, Ala 107, Pro 160, Leu 163, Cys 174	Ser 111
7NTH	Vitexin	-11.844	-53.282	Arg 44, Ala 107, Pro 160	Val 42, Ala 46, Val 50, Ala 61, Val 90, Met 104, Tyr 106, Ala 107, pro 160, Leu 163, Cys 174	Ser 111
7NTH	Apigenin	-9.277	-49.012	Val 42, Ala 107	Val 42, Val 50, Ala 61, Val 90, Met 104, Tyr 106, Ala 107, Leu 163, Cys 174	-
7NTH	Harman	-5.587	-38.578	Ala 107	Val 42, Val 50, Ala 61, Val 90, Met 104, Tyr 106, Ala 107, Leu 163, Cys 174	-
5R8Q	Orientin	-7.078	-44.091	Tyr 24, Glu 25, Val 132	Pro 23, Tyr 24, Leu 26, Leu 80, Leu 82, Pro 131, Val 132, Phe 133	Ser 21, Thr 79, Gln 81
5R8Q	Vitexin	-7.029	-44.036	Tyr 24, Glu 25	Pro 23, Tyr 24, Leu 26, Leu 80, Leu 82, Pro 131, Val 132, Phe 133	Ser 21, Thr 79, Gln 81
5R8Q	Apigenin	-5.293	-39.896	Tyr 24, Leu 134	Tyr 24, Leu 26, Leu 69, Pro 78, Leu 80, Leu 82, Trp 120, Val 132, Phe 133, Leu 134	Thr 79, Gln 81
5R8Q	Harman	-3.130	-32.346	Tyr 24	Tyr 24, Leu 26, Leu 69, Leu 80, Leu 82, Val 132, Phe 133, Leu 134	Thr 79, Gln 81
3NVY	Orientin	-8.985	-33.194	Lys 771, Ser 876, Glu 879	Leu 648, Phe 649, Leu 873, Phe 914, Phe 1009, Val 1011, Phe 1013, Leu 1014	His 875, Ser 876
3NVY	Vitexin	-8.014	-34.359	Glu 802, Glu 879	Leu 648, Phe 649, Leu 873, Phe 914, Phe 1009, Val 1011, Pro 1012, Phe 1013, Leu 1014, Phe 1142	His 875, Ser 876, Thr 1010
3NVY	Apigenin	-9.668	-45.574	Arg 880, Thr 1010	Leu 648, Phe 649, Leu 873, Phe 914, Phe 1009, Val 1011, Phe 1013, Leu 1014, Pro 1076, Ala 1078, Ala 1079	Ser 876, Thr 1010
3NVY	Harman	-5.548	-40.263	-	Leu 648, Phe 649, Leu 873, Phe 914, Ala 1009, Val 1011, Phe 1013, Leu 1014, Ala 1078, Ala 1079	Asn 768, Thr 803, Ser 876, Thr 1010

The four phytoconstituents shows considerable docking score and binding free energy against the PDB ID: 3NVY were found to be Orientin (-8.985 kcal/mol, -33.194 kcal/mol), Vitexin (-8.014 kcal/mol, -34.359 kcal/mol), Apigenin (-9.668 kcal/mol, -45.574 kcal/mol), and Harman (-5.548 kcal/mol, -40.263 kcal/mol). Except Harman all the compounds had the docking score of above -8.000 kcal/mol which typically tells that they have the optimum interaction with the binding site. Glu 879 was found to be the most common amino acid which is responsible for the H-bond formation. Leu 648, Phe 649, Leu 873, Phe 914, Phe 1009, Val 1011, Pro 1012, Phe 1013, Leu 1014, and Phe 1142 were the most common hydrophobic interactions forming amino acids present in the binding pocket. 876, Thr 1010 were the amino acids accountable for the polar interactions. In some cases, the Phe 914, Phe 1009 and Phe 1013 were shown to form the Pi-pi stacking (Figure 3).

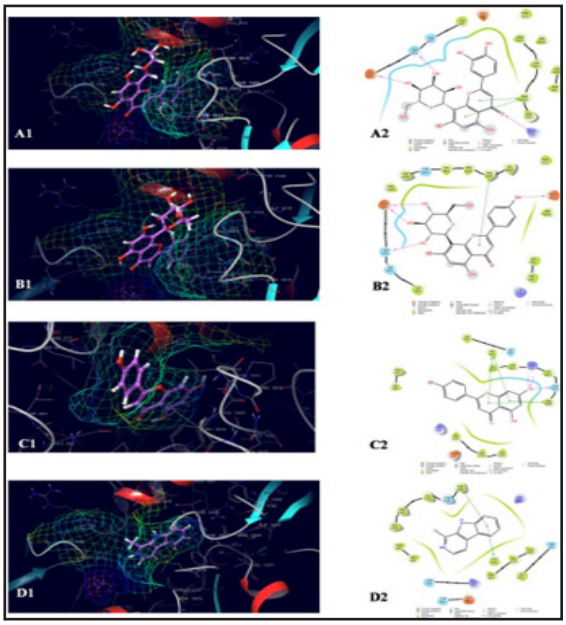

Figure 3. Molecular docking interactions of phytoconstituents in the binding pocket of PDB ID: 3NVY. (3D and 2D representation of Orientin (A1, A2), Vitexin (B1, B2), Apigenin (C1, C2), and Harman (D1, D2) in the binding pocket of (PDB ID: 3NVY))

Superimposition of the best docked pose of all four compounds into the binding pockets of TAK1, Interleukin-1 beta, and Xanthine Oxidase enzymes are depicted in the Figure 4 ((A), (B), and (C), respectively), exhibiting the fitness of these compounds into these enzymes' active pockets. The strong to moderate binding affinities possessed by these compounds against the three enzymes may lead to modulation of the enzymes.

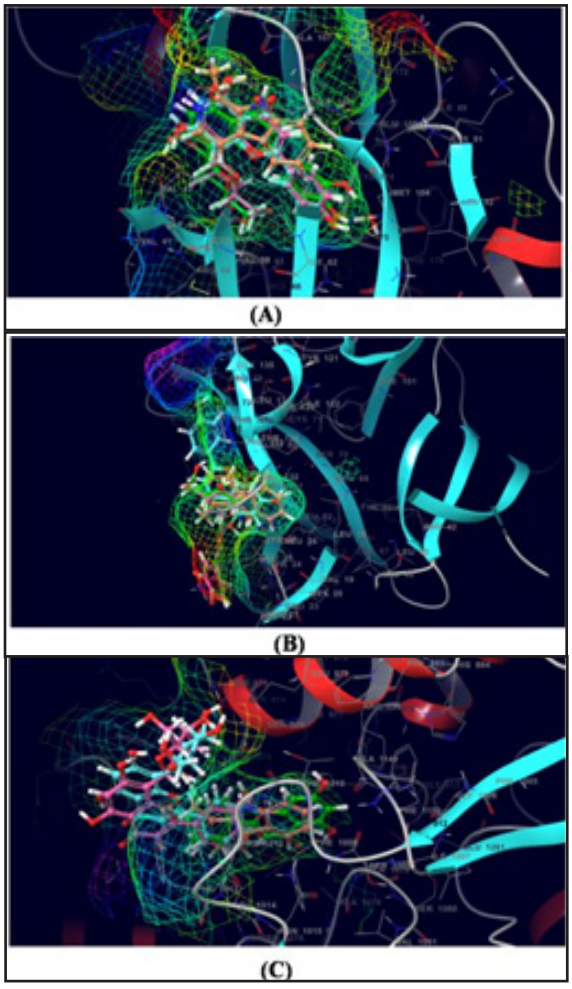

Figure 4. Superimposition of the best docked pose of Orientin, Vitexin, Apigenin, and Harman in the binding pocket of TAK1 (PDB ID: 7NTH) (A), Interleukin-1 beta (PDB ID: 5R8Q) (B), and Xanthine Oxidase (PDB ID: 3NVY) (C) respectively.

Molecular dynamics

The molecular docking studies stipulate the importance of the interacting amino acids which are mentioned above. For the insight study of the interactions there was a need for the molecular dynamics study of the best protein-ligand complexes which were performed for 100 ns of the simulation time.

For the better understanding of the solidity and visualization of the time span of the interacting amino acids in the dynamics condition the protein-ligand RMSD as well as protein–ligand contacts were explored. The validation of the stability of the receptor-ligand complex was done by performing molecular dynamics simulations using Desmond of Schrödinger 2017-2 for 100 ns.

Results revealed that Val 50, Lys 63, Ala 107, Gly 110, Pro 160, and Asp 17 etc. were found to be the important amino acids for binding of the ligands inside the binding pocket of the TAK1. The protein and ligand RMSD (Å) was found to be <1.2 Å which validates the stability of the analogue Orientin at the active site of the protein (PDB ID: 7NTH) (Figure 5A and 5B). During the starting of the simulation (0-40 ns and 80-100 ns), there was a bit of divergence (<1.2 Å). Moreover to demonstrate the protein–ligand stability the interactions were simulated for 100 ns. In the halfway of the simulation (40-60 ns) the protein ligand complex is exhibiting a negligible divergence. The amino acids Lys 63, Ala 107, Gly 110 and Pro 160 Tyr 290 were involved in the H-bonding for maximum simulation time of 0.3, 0.7, 0.5 & 0.4 fraction of time, respectively. Moreover, the important amino acids Val 50, and Ala 61 were involved in hydrophobic interactions for a fraction of 0.3. Glu 105, Pro 160, and Asp 175 were the amino acids responsible for water bridge formation for 0.7, 0.6, & 1.1 fractions of the total simulation time respectively (Figure 5C and 5D).

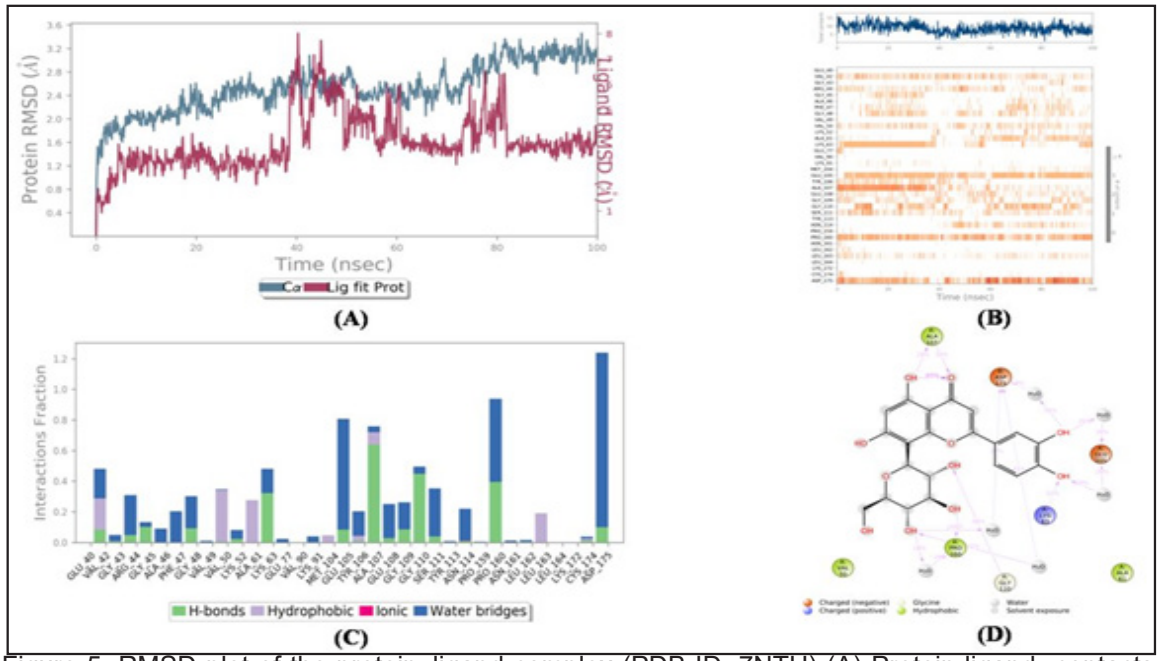

Figure 5. RMSD plot of the protein–ligand complex (PDB ID: 7NTH) (A) Protein-ligand contacts (B), stacked bar plot of the fraction of time of the interactions (C) and Ligand Protein contacts (D) of analogue Orientin for 100 ns of simulation time

In the case of Interleukin-1 beta (PDB ID: 5R8Q) the Orientin is interacting with the Tyr 24, Glu 25, Leu 26, Leu 80, Gln 81, Leu 82, Pro 131, Val 132, Phe 133, and Leu 134 in the binding site of the particular protein (PDB ID: 5R8Q). During the starting of the simulation (0-20 ns), the protein ligand complex is in very stable interactions. In the midway of the simulation (25-50 ns) there was a bit of divergence (<1.5 Å). Rest of the simulation time the divergence is <1.0 Å which is in considerable range. Moreover, to demonstrate the protein–ligand stability the interactions were simulated for 100 ns (Figure 6A and 6B). The amino acids Tyr 24, Glu 25, Leu 26, Gln 81, Leu 82, and Val 132 were involved in the H-bonding for a maximum simulation time of 0.8, 0.8, 0.85, 0.7, 0.75, & 0.9 fraction of time, respectively. Tyr 24, Lys 74, Pro 131, and Phe 133 were responsible for the hydrophobic interactions with simulation time of 0.2 fraction of time. Leu 80, Leu 134 were the amino acids responsible for the formation of weak water bridges with simulation time of 1.0 and 0.5 fraction of time respectively (Figure 6C and 6D).

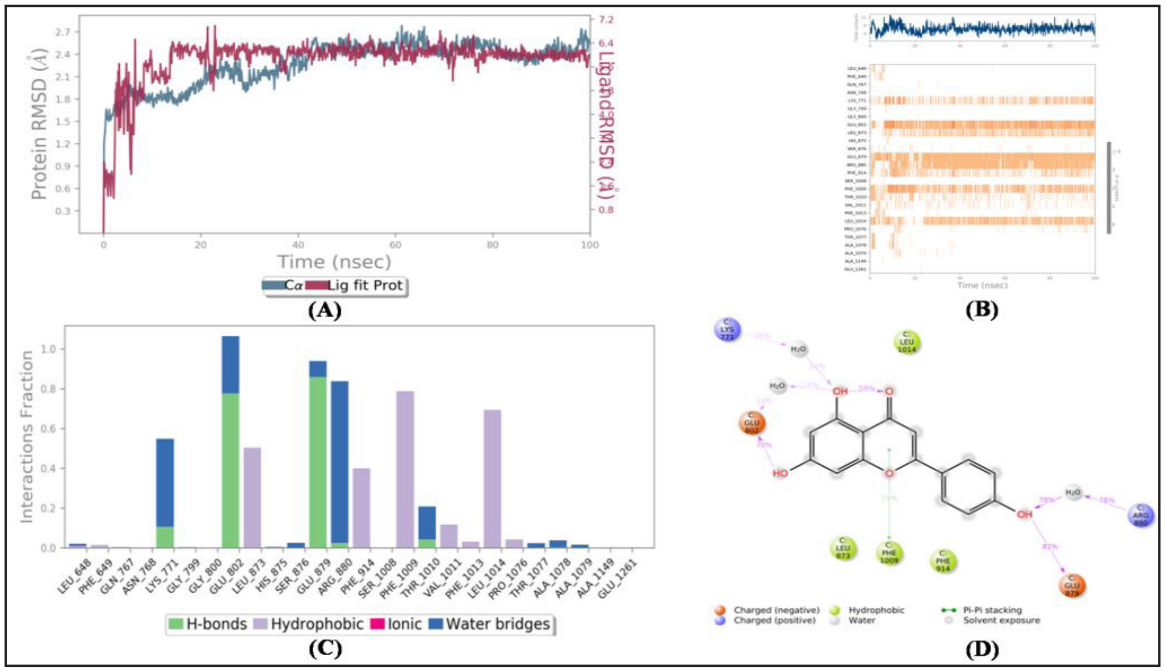

Figure 6. RMSD plot of the protein–ligand complex (PDB ID: 5R8Q) (A) Protein-ligand contacts (B), stacked bar plot of the fraction of time of the interactions (C) and Ligand Protein contacts (D) of analogue Orientin for 100 ns of simulation time.

In case of Xanthine Oxidase (PDB ID: 3NVY), the interacting amino acid residues with Apigenin were Lys 771, Glu 802, Leu 873, Glu 879, Arg 880, Phe 914, Phe 1009, and Leu 1014 etc. in the binding site. From the starting point till the completion of the whole simulation, the protein ligand complex was found to be highly stabilized except the 0-20ns where little divergence (< 0.6 Å) was reported. Glu 80 and Glu 879 were the H-bonding forming residues for maximum simulation time of 0.8 & 0.9 fraction of time, respectively. Leu 873, Phe 914, Phe 1009, and Leu 1014 were the hydrophobic residues for 0.5, 0.4, 0.8, & 0.7 fraction of time of the simulation study respectively. Additionally, Lys 771, Glu 802, and Arg 880 were the amino acids responsible for the water bridges formation for 0.4, 0.4 & 0.8 fraction of time of the simulation study (Figure 7).

Current Trends in Biotechnology and Pharmacy
Vol. 17(4) 1496-1505,October 2023, ISSN 0973-8916 (Print), 2230-7303 (Online)
DOI: 10.5530/ctbp.2023.4.83

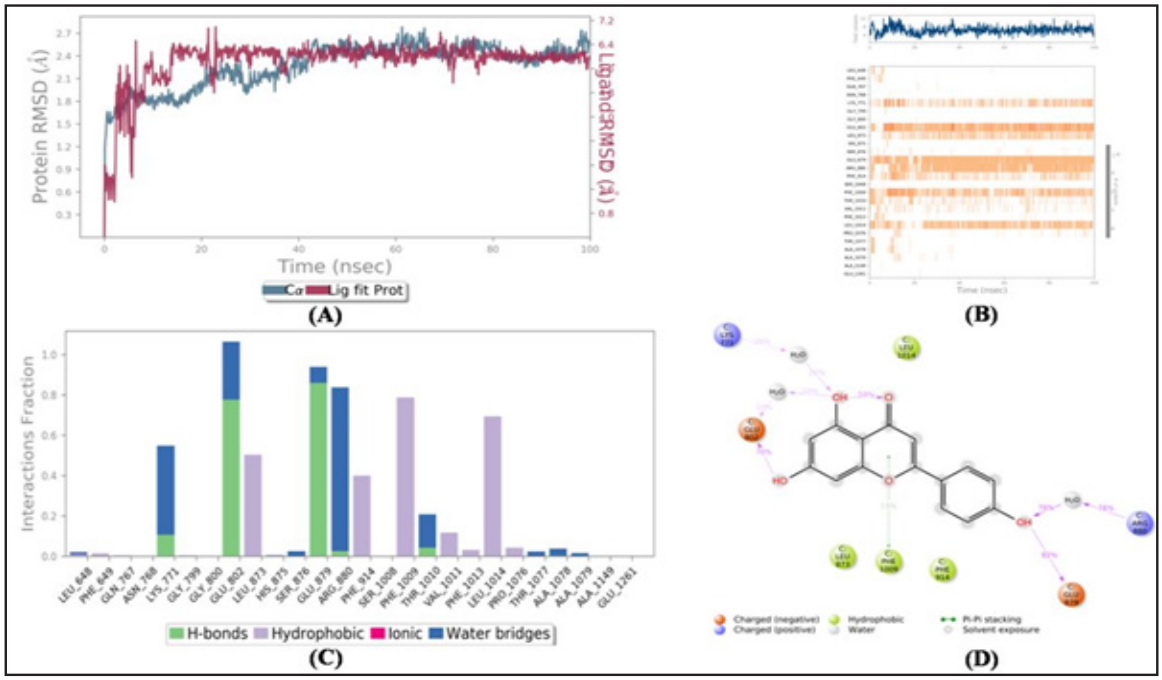

Figure 7. RMSD plot of the protein–ligand complex (PDB ID: 3NVY) (A) Protein-ligand contacts (B), stacked bar plot of the fraction of time of the interactions (C) and Ligand Protein contacts (D) of analogue Apigenin for 100 ns of simulation time.

***In silico* physicochemical and ADME/T studies**

The *in silico* physicochemical and pharmacokinetic properties of all the compounds, i.e Apigenin, Harman, Orientin, and Vitexin were predicted using the QikProp program of Schrödinger 2017-2 and the SwissADME online server, and are tabulated in Table 2. From the QikProp-predicted properties, all of them were found to be in the acceptable range for all the compounds. Also, all the compounds exhibited Log P, molecular weights, polarizability, solubility, and surface area within the acceptable range.

On the other hand, from the SwissADME-predicted properties, it can be found that among all the four compounds, only Harman was CNS-active. However, the same compound was found to be P-glycoprotein (PGP)-substrate, being responsible for the efflux of the foreign bodies from the human body (shown in egg-boiled diagram, Figure 8). All of the compounds showed no violations of Ghose's rule only except Orientin. Two compounds, i,e Orientin and Vitexin were not found to be CYP or cytochrome P450 enzymes (CYP1A2, CYP2C19, CYP2C9, CYP2D6, CYP3A4) inhibitors. Also, the other two compounds were not mostly CYP inhibitors.

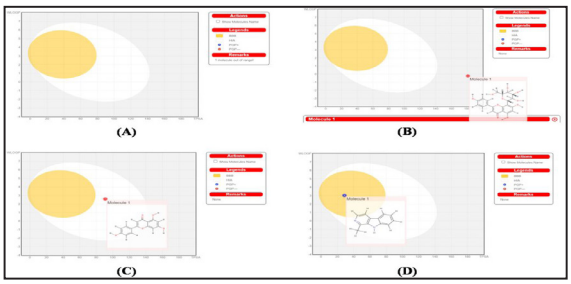

Figure 8. Egg boil diagram of Orientin (A), Vitexin (B), Apigenin (C), and Harman (D) imported from SwissADME. The molecule Orientin (A) was out of range.

Table 2. Physico-chemical properties and ADME/T profile

Molecule	Molecular Weight	SASA	PISA	Volume	QP polrz	QP log PC16	QP log P oct	QP logP w	QP logP o/w	QP log S	CI QP log S	QP log K hsa	CYP1A2 inhibitor	CYP2C19 inhibitor	CYP2C9 inhibitor	CYP2D6 inhibitor	CYP3A4 inhibitor
Orientin	448.382	669.846	190.162	1223.878	38.863	15.224	32.215	26.308	-1.308	-2.96	-4	-0.755	No	No	No	No	No
Vitexin	432.383	647.698	219.471	1197.24	38.719	14.601	30.105	24.127	-0.654	-2.996	-4.035	-0.622	No	No	No	No	No
Apigenin	270.241	490.278	285.959	818.082	27.39	9.674	15.53	10.195	1.607	-3.334	-4.101	-0.038	Yes	No	No	Yes	Yes
Harman	182.224	401.518	275.744	648.813	22.445	6.737	8.929	5.259	2.952	-3.179	-3.187	0.157	Yes	No	No	No	Yes

SASA - solvent-accessible surface area, PISA - Solute Carbon Pi SASA, QP polrz - QP Polarizability (Angstroms^3), QP logP C16 - QP log P for hexadecane/gas, QP logP oct - QP log P for octanol/gas, QP logP w - QP log P for water/gas, QP logP o/w - log P for octanol/water, Predicted QP log S - Predicted aqueous solubility, CI QP log S - Predicted conformation independent solubility, QP log K hsa - log K hsa Serum Protein Binding.

Conclusions

Orientin, Vitexin, and Apigenin except Harman all the three phytoconstituents showed a considerable docking score and MMGBSA score, which clearly indicates the possible interaction with the target proteins. ADME/T analysis indicated that the Vitexin, and Apigenin are satisfying the druglike molecule criteria. On the other hand the most potent Orientin and less potent Harman were missing some of the druglike molecule criteria.

References

1. Kuo, C.-F., et al., Global epidemiology of gout: prevalence, incidence and risk factors. Nature reviews rheumatology, 2015. 11(11): p. 649-662.

2. Narang, R.K. and N. Dalbeth. Pathophysiology of gout. in Seminars in Nephrology. 2020. Elsevier.

3. Yagnik, D.R., et al., Macrophage release of transforming growth factor β1 during resolution of monosodium urate monohydrate crystal–induced inflammation. Arthritis & Rheumatism: Official Journal of the American College of Rheumatology, 2004. 50(7): p. 2273-2280.

4. Martin, W.J., M. Walton, and J. Harper, Resident macrophages initiating and driving inflammation in a monosodium urate monohydrate crystal–induced murine peritoneal model of acute gout. Arthritis & Rheumatism, 2009. 60(1): p. 281-289.

5. Desai, J., S. Steiger, and H.-J. Anders, Molecular pathophysiology of gout. Trends in Molecular Medicine, 2017. 23(8): p. 756-768.

6. Dalbeth, N. and D. Haskard, Mechanisms of inflammation in gout. Rheumatology, 2005. 44(9): p. 1090-1096.

7. Ojha, R., et al., An updated patent review:

xanthine oxidase inhibitors for the treatment of hyperuricemia and gout (2011-2015). Expert opinion on therapeutic patents, 2017. 27(3): p. 311-345.

8. Sakurai, H., Targeting of TAK1 in inflammatory disorders and cancer. Trends in pharmacological sciences, 2012. 33(10): p. 522-530.

9. Totzke, J., et al., TAK1: a potent tumour necrosis factor inhibitor for the treatment of inflammatory diseases. Open Biology, 2020. 10(9): p. 200099.

10. Li, H., et al., Resveratrol attenuates the MSU crystal-induced inflammatory response through the inhibition of TAK1 activity. International Immunopharmacology, 2019. 67: p. 62-68.

11. Tatsiy, O., et al., Cytokine production and NET formation by monosodium urate-activated human neutrophils involves early and late events, and requires upstream TAK1 and Syk. Frontiers in immunology, 2020. 10: p. 2996.

12. Fechtner, S., D.A. Fox, and S. Ahmed, Transforming growth factor β activated kinase 1: a potential therapeutic target for rheumatic diseases. Rheumatology, 2017. 56(7): p. 1060-1068.

13. Kingsbury, S.R., P.G. Conaghan, and M.F. McDermott, The role of the NLRP3 inflammasome in gout. Journal of inflammation research, 2011. 4: p. 39.

14. So, A.K. and F. Martinon, Inflammation in gout: mechanisms and therapeutic targets. Nature Reviews Rheumatology, 2017. 13(11): p. 639-647.

15. Veerman, J.J., et al., Discovery of 2, 4-1 H-Imidazole Carboxamides as Potent and Selective TAK1 Inhibitors. ACS medicinal chemistry letters, 2021. 12(4): p. 555-562.

16. Nichols, C., et al., Mining the PDB for tractable cases where X-ray crystallography combined with fragment screens can Be used to systematically design protein–protein inhibitors: two test cases illustrated by IL1β-IL1R and p38α–TAB1 complexes. Journal of Medicinal Chemistry, 2020. 63(14): p. 7559-7568.

17. Cao, H., J.M. Pauff, and R. Hille, X-ray crystal structure of a xanthine oxidase complex with the flavonoid inhibitor quercetin. Journal of natural products, 2014. 77(7): p. 1693-1699.

18. Madhavi Sastry, G., et al., Protein and ligand preparation: parameters, protocols, and influence on virtual screening enrichments. Journal of computer-aided molecular design, 2013. 27(3): p. 221-234.

19. Shelley, J.C., et al., Epik: a software program for pK a prediction and protonation state generation for drug-like molecules. Journal of computer-aided molecular design, 2007. 21(12): p. 681-691.

20. Friesner, R.A., et al., Extra precision glide: Docking and scoring incorporating a model of hydrophobic enclosure for protein–ligand complexes. Journal of medicinal chemistry, 2006. 49(21): p. 6177-6196.

21. Bowers, K.J., et al. Scalable algorithms for molecular dynamics simulations on commodity clusters. in Proceedings of the 2006 ACM/IEEE Conference on Supercomputing. 2006.

22. Auti, P.S., et al., Design, synthesis, biological evaluation and molecular modelling studies of oxoacetamide warhead containing indole-quinazolinone based novel hybrid analogues as potential pancreatic lipase inhibitors. New Journal of Chemistry, 2022. 46(24): p. 11648-11661.